

# M acroscopic tunnel splittings in superconducting phase qubits

Philip R. Johnson, William T. Parsons, Frederick W. Strauch,<sup>y</sup>  
J.R. Anderson, Alex J. Dragt, C.J. Lobb, and F.C.W. Ellstodt

Department of Physics, University of Maryland, College Park, MD 20850  
(Dated: February 23, 2019)

Many prototype Josephson-junction based qubits have unacceptably short coherence times. Recent experiments probing a superconducting phase qubit with an extremely asymmetric double well potential have revealed previously unseen fine splittings in the transition energy spectra. These splittings have been attributed to new microscopic degrees of freedom (microresonators), a previously unknown source of decoherence. We show that the macroscopic resonant tunneling of states in an extremely asymmetric double well has some observational consequences that are strikingly similar to the observed data, suggesting a possible alternative explanation to microresonators. Our analysis indicates that macroscopic resonant tunneling may be unavoidable for double well phase qubits and thus must be taken into account.

PACS numbers: 74.50.+r, 03.67.Lx, 85.25.Cp

New experiments by Simmonds et al. [1] and Cooper et al. [2] have revealed previously unseen fine splittings in the transition energy spectra of superconducting qubits with extremely asymmetric double well potentials. These splittings have been interpreted to be the result of coupling between the circuit's collective dynamical variable (the superconducting phase describing the coherent motion of a macroscopic number of Cooper pairs) and microscopic two-level resonators, hereafter called microresonators [3], within Josephson tunnel junctions. Microresonators may be an important decoherence mechanism [1, 2, 4] for many different superconducting qubit devices [5, 6, 7], and may have broader implications for Josephson junction physics generally. Key questions remain however. Are the observed splittings truly a microscopic property of junctions? If so, can they be eliminated by improved fabrication techniques? Are they instead a macroscopic property of the particular circuit? Could the observed splittings be a combination of these two very different phenomena?

In fact, macroscopic resonant tunneling (MRT) in asymmetric double well systems, like the rfSQUID phase qubit, can produce spectral splittings by lifting degeneracies between the left and right well states. These effects have been probed by Rouse et al., Friedman et al., and others [8] in superconducting circuits involving tilted double wells with a few left well states, and ~10 right-well states. What is not obvious is that MRT effects can be important for extremely asymmetric double well potentials with hundreds or thousands of right well states. In this Letter, we analyze the rfSQUID qubit in this limit and show that MRT should produce some observational consequences that are strikingly similar to the observed data [1, 2]. MRT is therefore a possible alternative explanation to microresonators. Even if microresonators also exist, our theoretical analysis demonstrates that MRT has important physical implications for current experi-

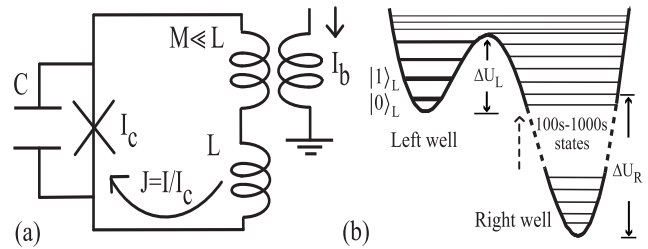


FIG. 1: (a) Circuit diagram for an rfSQUID qubit. (b) The device can be tuned via an inductively coupled bias line to give an extremely asymmetric double-well.

ments on double-well superconducting phase qubits.

Figure 1(a) shows the circuit schematic for an rfSQUID. The device is a superconducting loop of inductance  $L$  interrupted by a single Josephson junction with capacitance  $C$  and critical current  $I_c$ ; inductively coupled to a flux-bias line. Its dynamics is governed by the Hamiltonian

$$H = 4E_C p^2 - \omega^2 + E_J \cos \phi - J \quad ; \quad (1)$$

where  $\phi$  is the gauge invariant phase difference across the junction,  $p = \sim Q = 2e$  is the momentum conjugate to

$\phi$  (the charge on the plates of the capacitor),  $\omega = 2\pi I_c L / \hbar$  is the modulation parameter ( $\hbar = h/2e$  is the flux quantum), and  $J = I_c L / \hbar$  is the dimensionless current that is induced in the loop by the applied flux bias. The charging energy  $E_C = e^2/2C$  and Josephson energy  $E_J = I_c \phi_0 / 2e$  determine the regime of superconducting qubit behavior; for a phase qubit  $E_J \ll E_C$ :

The shape of the circuit's potential energy function  $V(\phi)$  depends on  $J$  and the bias  $J$ : For  $J \ll \omega$ , it is possible to bias the circuit so that the potential has the highly asymmetric double-well shape shown in Fig. 1(b), tuned to give a shallow upper left well with just a few

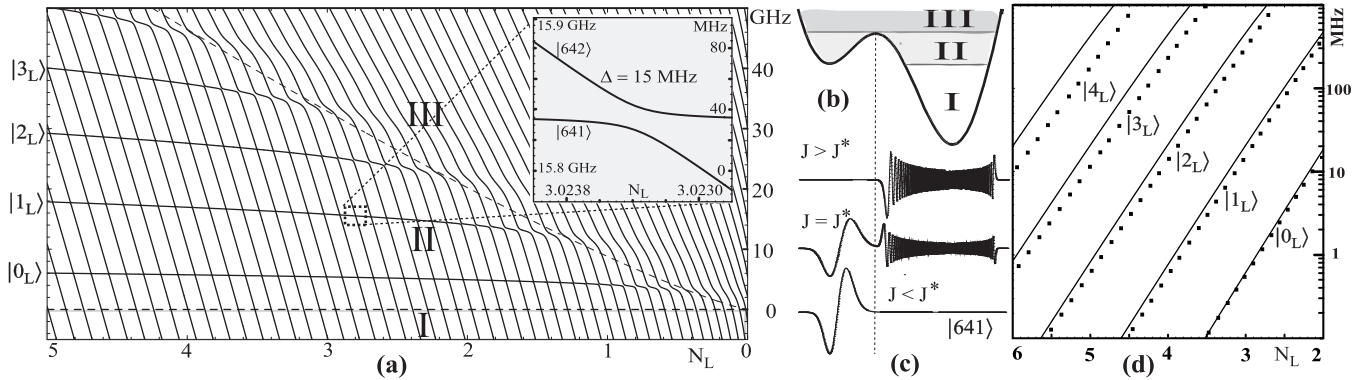


FIG. 2: (a) Numerically computed spectrum of phase qubit device when  $I_c = 8.35$  A,  $C = 12$  pF, and  $L = 168$  pH ( $\tau = 4.25$ ). Energies are plotted in units of frequency. The inset shows the avoided crossing due to resonant tunnel coupling between the left well state  $|1_L\rangle$  and a highly excited right well state. (b) The circuit parameters give an asymmetric double well like that shown. (c) Wavefunctions of the  $k = 641$  eigenstate for bias values near the avoided crossing shown in the inset. (d) Solid points are numerically computed sizes and locations of the splittings. Solid lines are splitting sizes derived from WKB theory.

left-localized states, denoted by  $|j_L\rangle$ , and a deep right well with many right-localized states, denoted by  $|j_R\rangle$ : We label states that are defined with respect to the two wells considered separately with the subscript L or R to distinguish them from full eigenstates of the double-well system. Simmonds et al. [1] (motivated by a number of attractive features (including reduced quasiparticle generation, inductive isolation from and reduced sensitivity to bias noise, and nice read-out properties) have proposed using the rfSQUID with an extremely asymmetric double well potential as a phase qubit [5].

Making a cubic approximation to the Hamiltonian, the frequency for small oscillations of in the left-well (i.e. the plasma frequency) is

$$\omega_L = \omega_0 \left( 1 - \frac{2}{3} \frac{1=8}{(2(J - J_c))^{1=4}} \right); \quad (2)$$

where  $\omega_0 = \sqrt{\frac{8E_c E_J}{\pi^2}}$ ; and

$$J_c = 1 - \frac{2}{3} \frac{1=2}{\omega_0^2} + \frac{1}{\omega_0} \arccos \frac{1}{\omega_0} > 1 \quad (3)$$

is the critical bias for which the left well vanishes. Note that the effective critical current is  $I = I_c J_c > I_c$ : The approximate number of left-well states is

$$N_L = \frac{U_L}{\omega_L}, \quad \frac{2^{3=4}}{3} \frac{r}{E_J} \frac{1}{E_C} \left( 1 - \frac{2}{3} \frac{1=8}{(J - J_c)^{5=4}} \right); \quad (4)$$

where  $U_L$  is the barrier height. The level spacing in the right well is approximately  $\sim \omega_R$ ; where  $\omega_R$  is the right well plasma frequency, and the number of right-well states is approximately  $N_R \sim U_R = \omega_R$ ; where  $U_R$  is the depth of the right well.

Figure 2(a) shows the energy spectrum as  $J$  is varied for  $0 \leq N_L \leq 6$  and  $C = 12$  pF,  $L = 168$  pH, and  $I_c = 8.531$  A, giving  $\tau = 4.355$  and  $I = 11.659$

A. These are the circuit parameters from [1], assuming that the critical current quoted there is  $I_c = 9$  A. To obtain the energy spectrum we diagonalize the Hamiltonian in Eq. (1) using a discrete Fourier grid representation [10], thereby obtaining a numerical solution for the eigenvalues [denoted  $E_k(J)$ ] and eigenstates [denoted  $|k(J)\rangle$ ] of the full double-well system versus the bias  $J$ . A harmonic approximation to the right well yields approximately 500 states below the left well; the full calculation yields  $N_R \sim 600 - 700$  states, depending on the bias [11].

In Fig. 2(a) we define the zero of energy to be at the bottom of the left well. We note two different types of energy levels: horizontal (H) branches and near vertical (V) branches. From our definition of zero energy, eigenvalues corresponding to states mainly localized in the right well [region I of Figs. 2(a) and (b)] fall with increasing  $J$ ; and are thus nearly vertical. The energy levels in region III correspond to delocalized states that are fully above the left well. The dashed line in Fig. 2(a) dividing regions II and III indicates the energy at the top of the left-well barrier.

In region II, eigenstates whose energies lie along H branches are primarily localized in the left well ( $H \subset L$ ). The number of stable left-well states at bias  $J$  is consistent with the estimate  $N_L$  from Eq. (4). Eigenstates whose energies lie along V branches are primarily localized in the right well ( $V \subset R$ ). Their energies fall at essentially the same rate as those in region I, i.e. with the rate of the falling right well. Note that in Fig. 2(a) the density of right-well states is comparable to that of the left-well, despite  $N_R \sim N_L$ :

Every apparent intersection of an H and V energy level in Fig. 2(a) is an avoided crossing (see inset). The degeneracies are lifted by resonant tunneling between left-well states  $|j_L\rangle$  and right-well states  $|j_R\rangle$ : Left of an avoided crossing between the  $k$  and  $k+1$  eigenstates we find that

$j_{ki} = j_{1i_L}$  and  $j_{k+1i} = j_{1i_R}$ . Right of the crossing the states swap, becoming  $j_{ki} = j_{1i_R}$  and  $j_{k+1i} = j_{1i_L}$ . At the avoided crossing  $j_{ki} = (j_{1i_L} + j_{1i_R})/2$  and  $j_{k+1i} = (j_{1i_L} - j_{1i_R})/2$ : Figure 2(c) shows the wavefunctions for the  $k = 641$  eigenstate before, at, and after the splitting shown in the inset in Fig. 2(a). Splitting magnitudes are plotted in Fig. 2(d) as solid points for the first five left-well states. Gaps larger than 1 MHz are within the resolution of recent experiments. Along each left-well energy branch the tunnel splittings are regularly spaced with magnitudes that decrease exponentially with  $N_L$ , a testable signature that should help distinguish tunnel splittings from microresonators.

The observational consequences of this collection of energy splittings are surprisingly complex. Consider a double frequency microwave spectroscopic method, like that used in [1]. Microwaves of frequency  $\omega_0$  are applied to drive the  $|0\rangle \rightarrow |1\rangle$  transition. Excitation of the  $|j_{1i_L}\rangle$  state is detected with a measurement microwave pulse of frequency  $\omega_{13}$ , which drives the  $|1\rangle \rightarrow |3\rangle$  transition. The  $|j_{1i_L}\rangle$  state has exponentially greater amplitude to be found in the right well compared to the  $|j_{1i_L}\rangle$  and  $|j_{1i_L}\rangle$  states, and an adjacent detection SQUID can easily measure the one-ux-quantum difference in the ux state of the qubit associated with right versus left well states. Thus the two-microwave method probes splittings of all three branches ( $|j_{1i_L}\rangle$ ,  $|j_{1i_L}\rangle$ , and  $|j_{1i_L}\rangle$ ) and generates a combined transition spectrum with a varied distribution of splittings sizes and bias-value locations which, due to its complexity, might appear to have a microscopic origin. Underlying regularities in the structure of the tunnel splitting spectra should allow experimental identification of splittings that have a resonant tunneling origin. We note that the predicted gap sizes [see Fig. 2(d)] are strikingly similar to those reported in [1, 2] (1–100 MHz). We have numerically computed spectra for a variety of circuit parameters, including  $I_c = 2$  A and  $C = 0.5$  pF which are comparable to those reported in [2]. In each case the spectrum looks similar to Fig. 2(a).

Measured with sufficient resolution, the shape of transition frequency avoided crossings due to MRT splittings should have distinctive characteristics. When driving the  $|0\rangle \rightarrow |1\rangle$  transition, a splitting in the  $|j_{1i_L}\rangle$  branch should produce a crossing like that shown in Fig. 3(a), whereas a splitting in the  $|j_{1i_L}\rangle$  branch should produce a crossing like that shown in Fig. 3(b). The observed shapes may be strongly dependent upon the experimental measurement technique. Any bias noise could smear out the splittings in the horizontal direction. For splittings in the lower energy branch [Fig. 3(a)] this would leave a distinct vertical frequency gap, but could give the observed splittings a horizontally smeared appearance like those observed in [1, 2]. In contrast, splittings in the upper branch [Fig. 3(b)] do not seem to be consistent with observation. Improved experimental resolution that re-

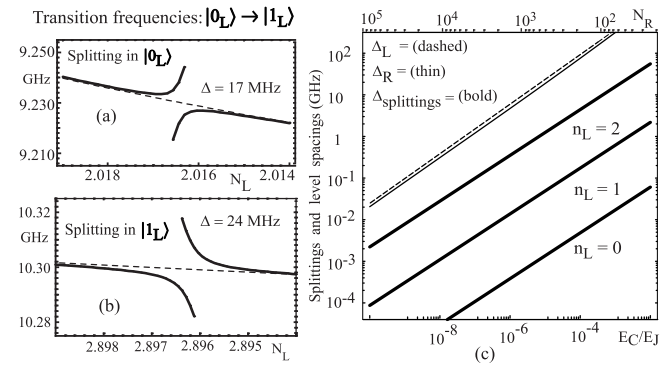


FIG. 3: (a) The distinctive shapes of avoided crossings in the measured transition frequencies for splittings in the lower branches. (b) The avoided crossing transition shape for splittings in the upper branch. (c) The figure shows that  $\Delta_L$  and  $\Delta_R$  over an extremely large range of double-well circuit parameters. Bold lines show the splitting magnitudes along the  $n_L = 0, 1$ ; and  $2$  left well energy branches, with  $n_R = 45$ ;  $N_L = 3$ ; and  $I_c = 10$  A.

vealed these distinctive avoided-crossing shapes would be compelling evidence for MRT and our understanding of the circuit. Han et al. have explored other complexities that arise when measuring systems that exhibit MRT [8].

An analytic expression for the energy splitting between pair-wise degenerate left and right states in an asymmetric double well can be derived in the WKB approximation [12]. This yields the splitting formula

$$\Delta = \frac{2 \pi \hbar}{m_R} \frac{n_L + \frac{1}{2}}{n_L n_R} \frac{m_R + \frac{1}{2}}{m_R + \frac{1}{2}} e^{-S}; \quad (5)$$

where  $S = \int_{x_{1,2}}^{x_{1,2} + p} \frac{dx}{2m(E - V(x))}$ ;  $m = C(\omega_0^2)^{1/2}$ ,  $x_{1,2}$  are the classical turning points for the barrier given by  $V(x_{1,2}) = E_{n_L}$ , and  $x_L \sim !_{L,R}$  are the left and right well level spacings at energy  $E_{n_L}$ . For deep right wells, Eq. (5) becomes independent of  $m_R$ : In this limit, together with the cubic approximation accurate for shallow left wells, the splittings are approximately

$$\Delta \sim \frac{2^{1/2} \pi}{n_L!^{3/2}} \frac{x_L}{x_R} (432N_L)^{\frac{n_L}{2} + \frac{1}{4}} e^{-\frac{18}{5}N_L}; \quad (6)$$

This result may be improved by using the WKB estimate  $\Delta_R = 2 \sim T_{cl}$  [13], where  $T_{cl}$  is the classical period of oscillation in the right well with energy  $E_{n_L}$ : The splittings calculated from Eq. (6) are shown as solid lines in Fig. 2(d). The agreement with the exact splittings (solid points) is excellent for lower lying left well states, and surprisingly good for the excited left-well states.

We have compared MRT splittings with Eq. (6) for a number of numerical examples with  $N_R = 100$ –1000; but in principle one can fabricate circuits with many thousands of right-well states. The WKB formula for

the splittings and level spacings allow the analysis of circuit parameters for very deep right wells where numerical treatment is impractical. Figure 3(c) shows  $\sim!_L$ ,  $\sim!_L$  (dashed line) and  $\sim!_R = 2 \sim!_{Cl}$  (solid line) versus the ratio  $E_C = E_J$  for  $I_c = 10 \text{ A}$ , a bias giving  $N_L = 3$ , and  $= 4.5$  just below the threshold where the potential develops three wells. (For the circuit parameters in Fig. 2 and [2],  $E_C = E_J = 10^4 - 10^6$ .) The specific value of  $I_c$  determines the frequency scale on the left of Fig. 3(c) but leaves the relative positions of the plotted lines essentially unchanged. The results are also insensitive to values restricted to the range yielding double well potentials. The top axis gives  $N_R$  from the harmonic oscillator approximation. The bold lines show the WKB splitting when  $n_L = 0, 1$ , and 2. We observe that validity conditions for two-state RT,  $\sim!_R$ ,  $\sim!_L$  and  $\sim!_{R,L}$ , are satisfied over a large range of circuit parameters and, neglecting the effects of dissipation for the moment, for  $N_R > 10^6$  and greater [14].

Dissipation suppresses resonant tunneling when  $R_R$  &  $R_R'$ ; where  $R_R \approx T_1$  is the width of excited right well states, and  $T_1$  is the dissipation time for  $j_{LR}$ !  $j_{LR}$  [15, 16]. Using the accurate WKB estimate for  $R_R$ ; we find the condition  $N_R \cdot j_L T_1$  for observing MRT. For a phase qubit with  $j_L = 2 \cdot 10$  GHz and  $T_1 = 10 \cdot 100$  ns, resonant tunneling should be detectable as long as  $N_R \cdot 600 \cdot 6000$  states. For the circuit parameters in Fig. 2  $N_R = 600 \cdot 700$  and for those in Fig. 3  $N_R = 150 \cdot 300$ , with a measured  $T_1' = 25$  ns. Thus, we do not believe that dissipation will remove the effects of MRT.

If the intrinsic dissipation is actually much smaller so that [6], it should be possible to observe coherent oscillations which could explain effects presently attributed to microresonators [2]. The existence of tunnel splittings could also be probed by tuning  $T_1$  through adjustable coupling to adjacent circuit elements.

Distinguishing tunnel splittings from microresonators will require more precise knowledge of circuit parameters, careful analysis of measurement techniques, and consideration of the effects of noise and dissipation. While phase qubits generally have some immunity to bias noise because the  $|0\rangle$  and  $|1\rangle$  states have nearly the same

ux expectation value, near degeneracies the eigenstates are more strongly effected by bias noise. This suggests that decoherence times will be reduced near splittings, which is consistent with observations [1, 2]. Coupling of the qubit ux to other degrees of freedom or external elements (e.g. an adjacent SQUID used to measure the change in the ux) should lead to enhanced dissipation of right-left oscillations. In contrast, the intrinsic influence of microresonators should not depend on external circuit elements, so one may use this behavior to help further distinguish between tunnel splittings and microresonators.

In conclusion, a complete understanding of rf SQ UID phase qubits should include the expected presence of tunnel splitting resonances. If the observed splittings are due

to a combination of M RT and m icroresonators, characterization of the m icroresonators will require first distinguishing them from M RT splittings. If instead m icroresonators fully explain the data, the failure to see tunnel splittings, at the resolution of present experiments, would itself require explanation. Finally, if resonant tunneling is confirmed{using the features we have described{it will have important design implications in regard to control, decoherence, state preparation, and m easurement, while opening up new prospects for studying m acroscopic quantum m echanics in superconductors.

This work was supported by the NSA, the NSF through the QUBIC program under grant number EIA 0323261, DOE grant DE-FG 02-96ER40949, and the State of Maryland through the Center for Superconductivity Research.

electronic address: philip@physics.um.edu

<sup>Y</sup> electronic address: fstrauch@physics.umd.edu

[1] R.W. Simmonds et al., *Phys. Rev. Lett.* **93**, 077003 (2004).

[2] K.B. Cooper et al., *Phys. Rev. Lett.* **93**, 180401 (2004).

[3] These have also been called spurious resonators, junction resonators, microstates, and critical current actuators, highlighting their possible association with critical current 1/f noise.

[4] D.J. Van Harlingen et al., *Phys. Rev. B* **70**, 064517 (2004); F.M. Fries and D. Loss, cond-mat/0408594 (2004).

[5] J.M. Martinis, S. Nam, J. Aumentado, and C. Urbina, *Phys. Rev. Lett.* **89**, 117901 (2002); Y. Yu et al., *Science* **296**, 889 (2002); A.J. Berkley et al., *ibid.* **300**, 1548 (2003); F.W. Strauch et al., *Phys. Rev. Lett.* **91**, 167005 (2003).

[6] T. Yamamoto et al., *Nature* (London) **425**, 941 (2003); Yu.A. Pashkin et al., *ibid.* **421**, 823 (2003); A.W. Alvarado et al., *ibid.* **431**, 162 (2004); D. Vion et al., *Science* **296**, 886 (2002).

[7] C.H. van der Wal et al., *Science* **290**, 773 (2000); I. Chiorescu, Y. Nakamura, C.J.P.M. Harmans, and J.E. Mooij, *Nature* (London) **299**, 1869 (2003); A. Izmailov et al., *Phys. Rev. Lett.* **93**, 037003 (2004); Y. Yu et al., *ibid.* **92**, 117904 (2004); L. Tian, S. Lloyd, and T.P.O. Orlando, *Phys. Rev. B* **67**, 220505(R) (2003).

[8] R. Rouse, S. Han and J.E. Lukens, *Phys. Rev. Lett.* **75**, 1614 (1995); S. Han, R. Rouse, and J.E. Lukens, *ibid.* **84**, 1300 (2000); J.R. Friedman et al., *Nature* (London) **406**, 43 (2000); D.V. Averin, J.R. Friedman, and J.E. Lukens, *Phys. Rev. B* **62**, 11802 (2000).

[9] If the value given in [1] is the intrinsic  $I_c$  of the junction the potential would have three rather than two wells; this would have many of the same features described here.

[10] C.C. Marston and G.G. Balint-Kurti, *J. Chem. Phys.* **91**, 6 (1989).

[11] These numbers disagree with the estimate  $N_R$  given in Fig. 1(b) of [1]. 2500

[12] The WKB formula given here was derived based upon methods described in A. Garg, *Am. J. Phys.* **68**, 430 (2000), and references therein. We used Herring's formula, assumed a WKB-form wavefunction under the bar-

rier, and matched onto excited harmonic oscillator wavefunctions in the two wells. See also J.M. Schmidt, A.N. Cleland, and J. Clarke, Phys. Rev. B 43, 229 (1991).

[13] L.D. Landau and E.M. Lifshitz, *Quantum mechanics: non-relativistic theory*, volume III, Pergamon Press (London) 1965.

[14] The continuum tunneling regime may be approached by increasing  $n_L$  to give a wide, many-welled potential, thereby decreasing  $n_R$  relative to  $n_L$ : For  $n_L \gg 1$ , e.g. a current-biased junction, the WKB tunneling rates are

$$\text{tunneling} = \frac{!_L}{2^n L!} (432n_L)^{n_L+1/2} e^{-\frac{36}{5}n_L} :$$

Note that the tunnel splitting formula in Eq. (6) predicts

splittings exponentially larger than continuum tunneling rates:  $\text{splitting} = \text{tunneling} \exp(18n_L) = 5$ :

[15] A.O. Caldeira and A.J. Leggett, Ann. Phys. (New York) 149, 374 (1983).

[16] A. Garg, Phys. Rev. B 51, 15161 (1995).

[17] It is interesting to speculate that unexpectedly short dissipation times of  $\sim 25$  ns in [2] result from damping of excited right well states, such that  $T_{\text{measured}} = T_1 = n_R$ : This would imply a  $T_1$  of a few s, consistent with expected relaxation times for these qubits (see footnote [11] in [2]).